MATEC Web of Conferences **1**, 04003 (2012)
DOI: 10.1051/matecconf/20120104003

Frequency shift and hysteresis suppression in contact-mode AFM using contact stiffness modulation

I. Kirrou, M. Belhaq

Laboratory of Mechanics, University Hassan II-Casablanca, Morocco

Abstract. In this paper the frequency response shift and hysteresis suppression of contact-mode atomic force microscopy is investigated using parametric modulation of the contact stiffness. Based on the Hertzian contact theory, a lumped single degree of freedom oscillator is considered for modeling the cantilever dynamics contact-mode atomic force microscopy. We use the technique of direct partition of motion and the method of multiple scales to obtain, respectively, the slow dynamic and the corresponding slow flow of the system. As results, this study shows that the amplitude of the contact stiffness modulation has a significant effect on the frequency response. Specifically, increasing the amplitude of the stiffness modulation suppresses hysteresis, decreases the peak amplitude and produces shifts towards higher and lower frequencies.

1 Introduction

In atomic force microscopy (AFM) [1], a micro-scale cantilever beam with a sharp tip is employed to scan the topography of a specimen surface. Typically, the contact-mode AFM is used in such applications to confine the surface force to a Hertzian contact regime between the tip and the moving surface. The performance of this contact-mode AFM in scanning requires the contact-mode regime to be maintained during the scan in order to obtain quantified results in terms of vibrational amplitude and amplitude response. However, it is known that in macro-scale mechanisms, contact-mode in the forced Hertzian contact regime is of softening-type. Further, for a slight increase of the amplitude of the harmonic excitation, contact losses occur near resonances and followed by a succession of impacts causing the deterioration of the device [2]. This loss of contact phenomenon has been observed for an idealized preloaded and non-sliding dry Hertzian contact modelled by a single-degree-of-freedom (SDOF) system [3]. Based on numerical simulations, analytical approximation and experimental testing [3,4], it was concluded that the loss of contact is generally initiated by jumps near the resonances. In order to control the location of such jumps, three strategies were developed recently [5,6]. The first strategy introduced a fast harmonic excitation added to the basic harmonic forcing from above, the second used a fast harmonic base displacement, while the third one considered a rapidly harmonic parametric stiffness. It was concluded that a fast harmonic base displacement causes the resonance curves to shift left, whereas the rapidly parametric stiffness shifts them right, offering thereby a method for controlling contact losses and impact trigging in the system.

The present work is focused on the effect of contact stiffness vibration of a contact-mode AFM on the frequency response, and consequently contact losses. This parametric vibrations in a Hertzian contact-mode AFM can be excited, for instance, by laterally vibrating the cantilever at its clamped end or by modulation of the Hertz coefficient which may be caused when the tip is scanning along certain directions [7].

Based on the fact that the first mode is predisposed to lose contact promptly with a slight change of parameters [8], attention will be restricted to the analysis of the response to the first mode of the microbeam. Namely, we consider a SDOF system modelling the cantilever dynamics of contact-mode AFM based on the Hertzian contact formulation. Indeed, although the response of AFM cantilever is highly nonlinear and difficult to explore, a SDOF model is often adopted to model the cantilever neglecting the higher-order flexural modes.

The rest of the paper is organized as follows: Section 2 presents a lumped SDOF model where the tip-sample interaction force is supposed to be in a Hertzian contact condition and in which the Hertzian coefficient is assumed to vary harmonically in time with a HF excitation. The method of direct partition of motion is applied to obtain the main equation of motion describing the slow dynamic of the tip-sample system. In Section 3, the method of multiples scales(MMS)is implemented on the slow dynamic equation to derive the corresponding slow flow near primary resonance. This Section includes results of various parameters effect on the frequency response and hysteresis. Section 4 concludes the work.

2 Model and slow dynamic equation

A representative model of a harmonically modulated contact-mode AFM operation is proposed. It consists of a lumped parameter SDOF model, as shown in Fig. 1 [9], described by the equation

$$m\ddot{x}+c_1\dot{x}+kx=-(k_0+k_1\cos\Omega_2 t)(z_0-x)^{\frac{3}{2}}+mg+F\cos\Omega_1 t \quad (1)$$

where x denotes the effective displacement of the cantilever tip, m is the lumped cantilever mass, c_1 $(= c_0 + c_*)$ the effective damping constant, k the free cantilever stiffness, k_0 the unmodulated Hertz coefficient, k_1, Ω_2 the amplitude

and high-frequency of the modulated Hertz coefficient, z_0 the surface offset, g the acceleration gravity, and F, Ω_1 are, respectively, the amplitude and the frequency of the sample vibration, as usually considered in atomic acoustic microscopy [10,11]. The displacement x is defined by considering the static problem as $x = x_s + X$, and the quantity $\Delta = z_0 - x_s$ as the static Hertz deformation, where x_s is the static position and X is the displacement from the static position. Introducing the variable changes as $u = \frac{X}{\Delta}$, $\tau = \omega_0 t$, $\omega_0^2 = \frac{k}{m}$, $c = \frac{c_1}{m\omega_0}$, $\beta = \frac{3k_0\Delta^{\frac{1}{2}}}{2m\omega_0^2}$, $\beta_1 = \frac{\beta}{4}$, $\beta_2 = \frac{\beta}{24}$, $f = \frac{F}{m\omega_0^2\Delta}$, $\omega = \frac{\Omega_1}{\omega_0}$ and $\Omega = \frac{\Omega_2}{\omega_0}$, the dimensionless equation of motion takes the form

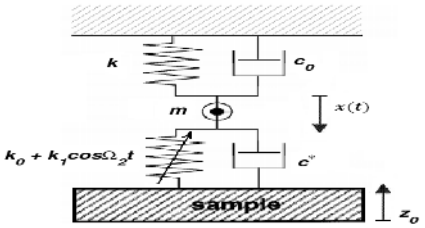

Fig. 1. A shematic of SDOF model of a tip-sample AFM (from [9]).

$$\ddot{u} + c\dot{u} + u - \frac{2}{3}\beta + \frac{2}{3}\beta(1 + r\cos\Omega\tau)(1-u)^{\frac{3}{2}} = f\cos\omega\tau \quad (2)$$

where $\dot{(\,)} = \frac{d}{d\tau}$ and $r = \frac{k_1}{k_0}$ is the ratio between the modulated and the unmodulated Hertz coefficients such that r takes values less than 1 ($k_1 < k_0$) or of order 1 ($k_0 \approx k_1$). Expanding the nonlinear restoring force in Taylor series around the static load and neglecting terms of order greater than three in u, Eq. (2) reads

$$\ddot{u} + \varpi^2 u + c\dot{u} + \beta_1 u^2 + \beta_2 u^3 + r(\frac{3}{2}\beta - \beta u + \beta_1 u^2 + \beta_2 u^3)\cos\Omega\tau = f\cos\omega\tau \quad (3)$$

where $\varpi = \sqrt{1-\beta}$ is the natural frequency. Equation (3) contains a slow dynamic due to the external excitation of the sample and a fast dynamic produced by the frequency of the parametric contact stiffness, Ω. Assume that the natural frequency, ϖ, may be in resonance with the external excitation, ω, but not in resonance with Ω (supposed larger than ϖ). Further, in order to keep ϖ small comparing to Ω, values of β have to be chosen as close as possible to 1 with the condition $\beta < 1$ to be satisfied. Taking these remarks into consideration, the effect of the parametric excitation on the slow dynamic can be investigated performing the method of direct separation of motion [12,13]. This method consists in introducing two different time scales, a fast time $T_0 = \Omega\tau$ and a slow time $T_1 = \tau$, and splitting up $u(\tau)$ into a slow part $z(T_1)$ and a fast part $\psi(T_0, T_1)$ as

$$u(\tau) = z(T_1) + \psi(T_0, T_1) \quad (4)$$

where z contains a slow dynamic which describes the main motions at time-scale of the tip natural vibrations and ψ stands for an overlay of the fast motions at time scale of the parametric excitation. The fast part ψ and its derivatives are assumed to be $2\pi-$periodic functions of fast time T_0 with zero mean value with respect to this time, so that $< u(t) >= z(T_1)$ where $<>\equiv \frac{1}{2\pi}\int_0^{2\pi}()\,dT_0$ defines time-averaging operator over one period of the fast excitation with the slow time T_1 fixed. Introducing $D_i^j \equiv \frac{\partial^j}{\partial^j T_i}$ yields $\frac{d}{dt} = \Omega D_0 + D_1$, $\frac{d^2}{dt^2} = \Omega^2 D_0^2 + 2\Omega D_0 D_1 + D_1^2$ and substituting Eq. (4) into Eq. (3) give the main equation governing the slow dynamic of the motion

$$\ddot{z} + \omega_1^2 z + c\dot{z} + \rho_1 z^2 + \rho_2 z^3 + H = f\cos\omega\tau \quad (5)$$

where the parameters ω_1^2, ρ_1, ρ_2 and H are given, respectively, by

$$\omega_1^2 = \varpi^2 + \frac{2\beta^2 r^2}{3\Omega^2} - \frac{5\beta^3 r^2}{36\Omega^4} - \frac{\beta^4 r^4}{48\Omega^6} \quad (6)$$

$$\rho_1 = \frac{\beta}{4} - \frac{\beta^2 r^2}{3\Omega^2} + \frac{\beta^3 r^2}{12\Omega^4} + \frac{7\beta^4 r^4}{192\Omega^6} \quad (7)$$

$$\rho_2 = \frac{\beta}{24} - \frac{\beta^2 r^2}{48\Omega^2} + \frac{\beta^3 r^2}{36\Omega^4} - \frac{35\beta^4 r^4}{1152\Omega^6} \quad (8)$$

$$H = -\frac{\beta^2 r^2}{3\Omega^2} + \frac{\beta^3 r^2}{18\Omega^4} + \frac{\beta^4 r^4}{216\Omega^6} \quad (9)$$

3 Frequency response analysis

In this Section we investigate the frequency-response curve of the slow dynamic (5) applying the MMS [14,15] near the primary resonance and we examine the effect of various system parameters on the frequency response.

3.1 Case without contact stiffness vibration

In order that the cubic nonlinearity balances the effect of damping and forcing, we scale parameters in Eq. (5) as $c = \epsilon^2 c$, $\rho_2 = \epsilon^2\rho_2$ and $f = \epsilon^2 f$ (the other parameters being of order ϵ) so that they appear together in the modulation equations. Thus, Eq. (5) reads

$$\ddot{z} + \omega_1^2 z = -\epsilon(\rho_1 z^2 + H) - \epsilon^2(c\dot{z} + \rho_2 z^3 - f\cos\omega\tau) \quad (10)$$

To analyze the dynamic near the principal resonance, we express the resonance condition by introducing a detuning parameter σ according to

$$\omega = \omega_1 + \epsilon\sigma \quad (11)$$

To ultimately solve Eq. (5), steady-state solution are expanded as

$$z(T_0, T_1, T_2) = z_0(T_0, T_1, T_2) + \epsilon z_1(T_0, T_1, T_2) + \epsilon^2 z_2(T_0, T_1, T_2) + 0(\epsilon^3) \quad (12)$$

where $T_0 = \tau$, $T_1 = \epsilon\tau$ and $T_2 = \epsilon^2\tau$. Substituting (12) into (10), we obtain the following relation expressing the vanishing of secular terms

$$\rho_n A^2\bar{A} + \rho_l A + i(-2\omega_1 D_2 A - c\omega_1 A) + \frac{f}{2}e^{i\sigma T_2} = 0 \quad (13)$$

where

$$\rho_n = \frac{10\rho_1^2}{3\omega_1^2} - 3\rho_2, \qquad \rho_l = \frac{2\rho_1 H}{\omega_1^2} \quad (14)$$

are, respectively, the effective nonlinearity and the effective linearity induced by the contact stiffness vibration and $A(T_1)$ is a complex amplitude.

To better understanding the dynamic of the oscillating tip, the variation of these two quantities, ρ_n, ρ_l, will be examined shortly. Equation (13) can be solved for the complex amplitude by introducing its polar form as

$$A = \frac{1}{2} a e^{i\theta} \tag{15}$$

Consequently, the modulation equations of amplitude and phase can be extracted as

$$\begin{cases} \dfrac{da}{dt} = \dfrac{f}{2\omega_1} \sin\varphi - \dfrac{c}{2} a \\ \dfrac{d\varphi}{dt} = \dfrac{f}{2\omega_1} \cos\varphi + \left[\dfrac{5\rho_1^2}{12\omega_1^3} - \dfrac{3\rho_2}{8\omega_1^2} \right] a^3 + \left[\sigma + \dfrac{\rho_1 H}{\omega_1^3} \right] a \end{cases} \tag{16}$$

in which $\varphi = \sigma T_2 - \theta$. Periodic solutions of Eq. (5) correspond to stationary solutions of the modulation equations (16), i.e. $\dot{a} = \dot{\varphi} = 0$. These stationary solutions are given by the following algebraic equation

$$AJ^3 + BJ^2 + CJ + D = 0 \tag{17}$$

where $A = (\frac{3}{4}\rho_2 - \frac{5\rho_1^2}{6\omega_1^2})^2$, $B = 2c\omega_1(-2\omega_1\sigma - \frac{2\rho_1 H}{\omega_1^2})$, $C = (c\omega_1)^2 + (-2\omega_1\sigma - \frac{2\rho_1 H}{\omega_1^2})^2$, $D = -f^2$ and $J = a^2$. Next, the effect of excitation amplitude, f, and contact stiffness, β, is analyzed before the application of the parametric vibration ($r = 0$).

Figure 2 shows the variation of the amplitude-frequency response, as given by Eq. (17), for different values of the excitation amplitude f. The solid lines denote stable solutions and the dashed lines denote unstable ones. Results from direct numerical simulation of Eq. (5) (circles) using Runge-Kutta method are also plotted for validation. It can be seen from this figure large response amplitude, softening-type behavior and hysteretic jumps when f is increased. In terms of the quantities defined in the case of Hertzian contact, values of r greater than 1 mean loss of contact [8].

Figure 3 depicts the variation of the frequency response for different values of the contact stiffness β. The plots reveal that an increase of β leads to an increase in softening behavior. This phenomenon (also reported in [8] for a micro cantilever) shows that the contact stiffness has a significant effect on nonlinear characteristic of the system and consequently the analysis of the nonlinear behavior can provide important information on the tip-sample interaction.

3.2 Case with contact stiffness vibration

Now we consider the case where the contact stiffness modulation is introduced into the system ($r \neq 0$) and hereafter we fix the parameters $c = 0.02$ and $\beta = 0.8$. First, let us examine the roots of Eq. (17). Then, the effect of the amplitude, r, and frequency, Ω, of the contact stiffness modulation is examined. In Fig. 4 is illustrated the frequency-response curves for various values of r. By inspecting this

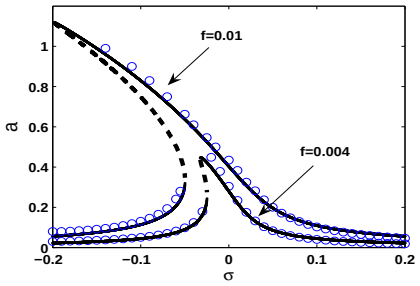

Fig. 2. Frequency-response curves for $r = 0$, $c = 0.02$, $\beta = 0.8$ and for different values of f. Analytical approximation (solid lines for stable, dashed lines for unstable) and numerical simulation (circles).

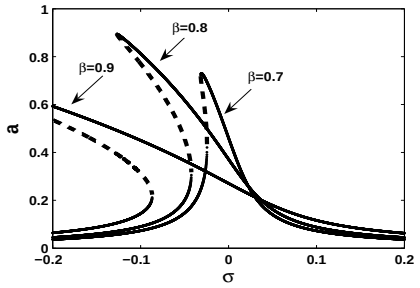

Fig. 3. Frequency response for $r = 0$, $c = 0.02$, $f = 0.008$ and for different values of β.

figure, it is evident to note the following phenomenon. Increasing r from 0.4 to 0.7, the amplitude response shifts toward higher frequencies while changing from softening to linear behavior. Increasing the amplitude r much more, the linear frequency response continues shifting right until reaching a maximum position for a certain critical value of r, and then shifts back toward lower frequencies (curve for $r = 1$). Note the substantial decreasing of the peak amplitude. Figure 5 shows in the parameter plane (r, Ω) the

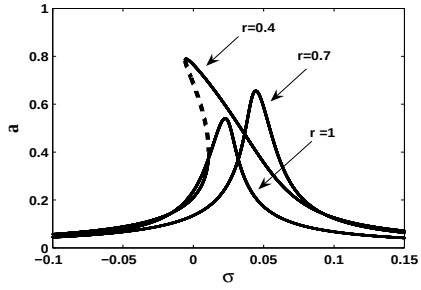

Fig. 4. Frequency response for $f = 0.008$, $\Omega = 1$ and different values of r (dots)).

boundary given by the condition (14) separating the regions where the frequency response is softening (region I) or linear (region II). It can be seen in this figure that in the presence of contact stiffness modulation ($r \neq 0$), and for appropriate values of r and Ω, the frequency response meets a linear behavior. The curves shown in the small boxes in Fig. 6 are obtained for values of r and Ω as given in the legend.

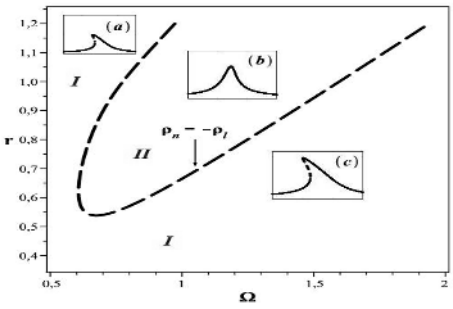

Fig. 5. Curve separating softening and linear domains of the response in the plan (r, Ω) for $f = 0.008$. In box (a): $\Omega = 0.6, r = 1$, (b): $\Omega = 1, r = 1$, (c): $\Omega = 1.5, r = 0.6$.

3.3 Application to a real AFM example

The mathematical model studied in the previous sections is compared with a real AFM example. Those comparisons are made using the parameters typical to those found in atomic-force microscopes [16]. The elastic modulus and density for silicon, $E = 169GPa$, $\rho = 2330kg/m^3$, respectively, were used. The cantilever has width $a = 51\mu m$, thickness $b = 1.5\mu m$, length $L = 262\mu m$, the lumped mass $m = 1.13 \times 10^{-11}kg$ and the free stiffness $k = 0.404N/m$. Also, the following parameters, corresponding to a single crystal silicon tip interacting with a chromium surface, were used in the numerical results that follow: $R = 20nm$, $\Delta = 0.26 \times 10^{-6}\mu m$, $E_t = 130GPa$, $\nu_t = 0.181$, $E_s = 204GPa$ and $\nu_s = 0.26$, where R is the tip radius, E_t, E_s are the elastic modulus of the tip and surface and ν_t, ν_s are poisson's ratio of the tip and surface respectively.
For comparison, we present in Fig. 6 the curve given by (14) in the plane (r, Ω). The solid line corresponds to the analytical approximation and the dashed line corresponds to the result given by the typical AFM example.

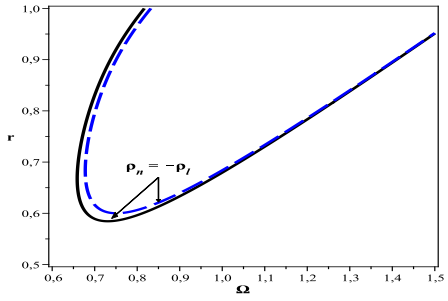

Fig. 6. Curve separating softening and linear domains of the response in the plan (r, Ω).

4 Conclusions

The effect of contact stiffness modulation on the frequency response of a contact-mode AFM was studied in this work. A lumped SDOF system modelling the cantilever dynamics of contact-mode AFM was considered and emphasis was placed on the case when the AFM is driven near primary resonance. The contact force was assumed as a modulated Hertzian contact model and the external harmonic force was derived from the sample vibration. The technique of direct separation of motion as well as the multiple scales technique were used to determine the nonlinear frequency response of the slow dynamic near the resonance.

The main results of this work is that for small values of damping, external forcing and contact stiffness, the hysteresis in contact-mode AFM, based on a lumped parameter SDOF model, can be eliminated under the effect of contact stiffness modulation.This allows the contact-mode AFM to be maintained such that a good performance of the AFM operation can be achieved in term of scanning or measuring proprieties of the specimen.

References

[1] Binnig G, Quate F, Gerber C. Atomic force microscope. Phys Rev Lett 1986;56:930-933.
[2] Sabot J, Krempf P, Janolin C. Nonlinear vibrations of a sphere plane contact excited by a normal load. J Sound Vib 1998;214:359-375.
[3] Perret-Liaudet J, Rigaud E. Response of an impacting Hertzian contact to an order-2 subharmonic excitation: Theory and experiments. J Sound Vib 2003;296:319-333.
[4] Perret-Liaudet J, Rigaud E. Response of an impacting Hertzian contact. Part 2: Random excitation: theory and experiments. J sound vib 2003;265:309-327.
[5] Bichri A, Belhaq M, Perret-Liaudet J. Control of vibroimpact dynamics of a single-sided Hertzian contact forced oscillator. Nonlinear Dyn 2010;63:51-60.
[6] Bichri A, Belhaq M. Control of a forced impacting Hertzien contact oscillator near-subharmonic and superharmonic of order 2. Comput Nonlinear Dyn 2011;7:011003. doi:10.1115/1.4004309.
[7] Xie HY. Frequency shift of cantilever in AFM. Applied Surface Science 2005; 252:372-378.
[8] Turner A. Non linear vibrations of a beams with cantilever hertzien boundary conditions. J Sound Vib 2004;275:177-191.
[9] Rabe U, Turner J, Arnold W. Analysis of the high-frequency response of atmic force microscope cantilevers. Appl Phys 1998;66:277-282.
[10] Rabe U, Janser K, Arnold W. Vibration of free and surface coupled atomic force microscopy cantilevers: theory and experiment. Rev Sci Instrum 1996;67:3281-93.
[11] Rabe U, Kester E, Arnold W. Probing linear and nonlinear tip-sample interaction forces by atomic force acoustic microscopy. Surf Interface Anal 1999;27:386-391.
[12] Blekhman II. Vibrational mechanics-nonlinear dynamic effects, general approach, application. Singapore: World Scientific 2000.
[13] Thomsen J.J. Vibrations and stability: Advanced Theory, Analysis, and Tools. Springer Berlin 2003.
[14] Nayfeh AH, Mook DT. Nonlinear Oscillations. New York: Wiley 1979.
[15] Nayfeh AH. Introduction to Perturbation Techniques. New York: Wiley 1981.
[16] Turner J.A, Hirsekorn S, Rabe U, Arnold W. High-frequency response of atomic-force microscope cantilevers. Appl. Phys 1997;82:966-979.